International Journal of Thermal Sciences 49 (2010) 187–195

Contents lists available at ScienceDirect

International Journal of Thermal Sciences

journal homepage: www.elsevier.com/locate/ijts

Experimental validation of model predictions on evaporator coils with an emphasis on fin efficiency

S.Y. Liang [a,b,**], T.N. Wong [a,*]

[a] School of Mechanical and Aerospace Engineering, Nanyang Technological University, Singapore 639798
[b] Technology Center, Henan Xinfei Electric Co. Ltd, XinXiang City, Henan, China, A Member of Hong Leong Group, Singapore

ARTICLE INFO

Article history:
Received 4 July 2008
Received in revised form
20 July 2009
Accepted 19 August 2009
Available online 22 September 2009

Keywords:
Evaporator modeling
Simultaneous heat and mass transfer
Wet fin efficiency
Experimental study

ABSTRACT

Simultaneous heat and mass transfers occur when an evaporator coil works in a wet condition due to the condensation of moist air. In evaporator modeling, overall fin efficiency is commonly used in heat balance and mass conservation equations to calculate sensible and latent heat transfers. In this paper, to analyze the simultaneous heat and mass transfer on the evaporator coils, a new concept, i.e. sensible and latent fin efficiencies, is introduced. The result shows that the latent fin efficiency is generally not equal to the sensible or the overall fin efficiencies. The proposed 1-D wet fin efficiency model has been validated by the extensive comparison of the model predictions against the experimental data on evaporator coils with various configurations that include simple and complex refrigerant circuitry.

1. Introduction

To make evaporator coils more compact and efficient, extended surface such as continuous plate fins made of aluminum or copper are added to the tube surface on the air side. The addition of fins to the tubes greatly increases the outer surface area but at an expense of decreasing the mean temperature difference between the surface and the air stream. Thus, fin efficiency is introduced to evaluate the heat transfer on the extended surface. Since the heat transfer mechanism encountered on the wet fins where simultaneous heat and mass transfer prevails is different from that on the dry fins, special attention is needed to the wet fin efficiency in evaporator coil simulation.

McQuiston [1,2] suggested a working dual-potential method introducing a C parameter to take into account the effect of the mass transfer, which was taken as a constant value determined by the moist air properties and the conditions at fin base. McQuiston method is widely employed [3–6]. However, it is noted that this analytical approach calculates the wet fin efficiency is based on a formula modified from a dry fin. These assume a linear variation of saturated humidity ratio with temperature [7–9]. Comparison of the models proposed by [8,9] shows that the results of McQuiston method are significantly different. The wet-surface fin efficiency predicted by McQuiston method decreases approximately linearly with the increase in air inlet relative humidity. McQuiston method fails to distinguish the difference between a partially wet fin and a totally wet fin, thus it gives much higher fin efficiency for a partially wet fin. In McQuiston method, a constant value of C is assumed based on the conditions at the fin base. In fact, the parameter C is not constant; it varies over the fin surface. At a high air relative humidity, this method under-predicts the fin efficiency due to the use of an unreasonably big C value at this condition.

In evaporator modeling, numerical distributed models are commonly used, where the evaporator coil is investigated based on numerous control volumes [3,4,10,11]. For each control volume, when simultaneous heat and mass transfers occur on the air side, both the energy and mass conservation equations are accordingly needed. Hence, the fin efficiencies for the sensible heat transfer and the mass transfer are needed in the computation. However, due to the lack of data, the overall fin efficiency obtained by McQuiston method is commonly used to calculate the sensible and latent heat transfer [3,4].

An effort to analytically study the evaporator coils with complex refrigerant circuitry under a humid environment is recently reported by the authors [10,11]. The present investigation extends the previous study both on theoretical modeling and the experimental validations. A main effort is made to modify the governing

* Corresponding author.
** Corresponding author. Technology Center, Henan Xinfei Electric Co. Ltd, XinXiang City, Henan, China.
E-mail addresses: borisliang@xinfei.com (S.Y. Liang), mtnwong@ntu.edu.sg (T.N. Wong).

1290-0729/$ – see front matter © 2009 Elsevier Masson SAS. All rights reserved.
doi:10.1016/j.ijthermalsci.2009.08.004

Nomenclature

A	heat transfer area (m^2)
C_p	isobaric specific heat (J kg^{-1} K^{-1})
d	tube diameter (m)
h	specific enthalpy (J kg^{-1})
i_{fg}	latent heat of moisture condensation (J kg^{-1})
k	thermal conductivity (W m^{-1} K^{-1})
L	tube length (m)
Le	Lewis number
m	mass flow rate (kg s^{-1})
Q	heat transfer rate (W)
r	fin radius (m)
t	fin thickness (m)
T	temperature (K)
ΔT_m	log mean temperature difference (K)
U_o	overall-heat-transfer coefficient (W m^{-2} K^{-1})
W	air specific humidity (kg kg^{-1})

Greek

α_{sen}	heat transfer coefficient (W m^{-2} K^{-1})
α_m	mass transfer coefficient (kg m^{-2} s^{-1})
δ	incremental element
ϕ	fin efficiency

Subscript

a	air
fb	fin base
d	dew point
f	fin
i	inner
in	inlet
lat	latent
o	outer
out	outlet
r	refrigerant
s	saturated
sen	sensible
t	tube
tot	total
w	water, wet

Abbreviation

HTC	heat transfer coefficient

equations of the model on the air side by introducing a latent-heat-transfer fin efficiency to compute the mass transfer. To validate the modified model, numerous experimental data are collected to compare with the model predictions.

2. Governing equations

A detailed evaporator model was presented previously based on numerous control volumes [10,11]. The governing equations for each control volume were provided along with the computation algorithm. Here, special attention is given to modify the air-side governing equations, in an attempt to reveal the heat and mass transfer mechanisms and hence to improve the model accuracy.

2.1. Air-side heat transfer equation

The computation in the model [10,11] is based on an arbitrarily small control volume, shown in Fig. 1. For a control volume, the heat transfer equation on the air side can be expressed as:

$$\begin{aligned}\delta Q_{tot} &= U_o(\delta A_t + \delta A_f)\cdot \Delta T_m = \delta Q_t + \delta Q_f \\ &= (\delta Q_{sen,t} + \delta Q_{lat,t}) + (\delta Q_{sen,f} + \delta Q_{lat,f})\end{aligned} \quad (1)$$

The heat transfer on the tube surface can be obtained by:

$$\delta Q_t = \delta A_t \cdot \left[\alpha_{a,sen}(T_a - T_{fb}) + \alpha_{a,m} i_{fg}(W_a - W_{s,fb})\right] \quad (2)$$

where $\alpha_{a,sen}$ and $\alpha_{a,m}$ are the air-side sensible-heat-transfer coefficient and mass transfer coefficient respectively. Using the heat and mass transfer analogy, the mass transfer coefficient $\alpha_{a,m}$ can be obtained by:

$$\alpha_{a,m} = \frac{\alpha_{a,sen}}{Le^{1-n}\cdot C_{p,a}} \quad (3)$$

Using overall fin efficiency ϕ, the heat transfer rate on the fins can be readily obtained once the conditions at the fin base are specified.

$$\delta Q_f = \phi\cdot\delta A_f\left[\alpha_{a,sen}(T_a - T_{fb}) + \frac{\alpha_{a,sen}\cdot i_{fg}}{Le^{1-n}\cdot C_{p,a}}(W_a - W_{s,fb})\right] \quad (4)$$

Thus, the heat transfer equation on the air side is expressed as:

$$\delta Q_{tot} = \alpha_{a,sen}(\delta A_t + \phi\delta A_f)\cdot\left[(T_a - T_{s,fb}) + \frac{i_{fg}}{Le^{1-n}\cdot C_{p,a}}(W_a - W_{s,fb})\right] \quad (5)$$

Introducing a mass transfer factor C,

$$C = \frac{W_a - W_{s,fb}}{T_a - T_{s,fb}} \quad (6)$$

Then, Equation (5) becomes:

$$\delta Q_{tot} = (\delta A_t + \phi\delta A_f)\cdot\left(\alpha_{a,sen} + \frac{i_{fg}\cdot\alpha_{a,sen}}{Le^{1-n}\cdot C_{p,a}}C\right)\cdot(T_a - T_{s,fb}) \quad (7)$$

Hence, for wet surface, the overall air-side heat transfer coefficient $\alpha_{a,w}$ can be expressed as:

$$\alpha_{a,w} = \alpha_{a,sen}\cdot\left(1 + \frac{i_{fg}\cdot C}{Le^{1-n}\cdot C_{p,a}}\right) \quad (8)$$

Thus, the overall-heat-transfer coefficient U_o in Equation (1) can be given as:

$$\begin{aligned}\frac{1}{U_o} &= R_a + R_t + R_r \\ &= \frac{\delta A_t + \delta A_f}{\alpha_{a,w}(\delta A_t + \phi\cdot\delta A_f)} + \frac{(\delta A_t + \delta A_f)\cdot(d_o - d_i)}{\pi(d_o + d_i)\delta z\cdot k_t} + \frac{(\delta A_t + \delta A_f)}{\delta A_i\alpha_r}\end{aligned} \quad (9)$$

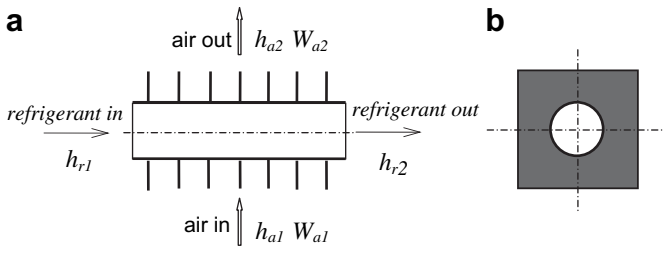

Fig. 1. A control volume along a tube with fins.

Consider the heat balance of the air,

$$\delta Q_{tot} = = \delta m_a(h_{a1} - h_{a2}) - h_w \cdot \delta m_a \cdot (W_{a1} - W_{a2}) \quad (10)$$

From Equations (7) and (10), the heat transfer equation of the air side is finally obtained:

$$\delta m_a h_{a2} = \delta m_a h_{a1} - \alpha_{a,sen}(\delta A_t + \phi \delta A_f) \cdot \left[(T_a - T_{fb}) + \frac{i_{fg}}{Le^{1-n} \cdot C_{p,a}} (W_a - W_{s,fb}) \right] - C_{p,w} T_{fb} \delta m_a (W_{a1} - W_{a2}) \quad (11)$$

2.2. Air-side mass transfer equation

Using the heat and mass transfer analogy, the mass transfer governing equation is given by:

$$\delta m_a W_{a2} = \delta m_a W_{a1} - \frac{\alpha_{a,sen}}{C_{p,a} Le^{1-n}} (\delta A_t + \phi_{lat} \cdot \delta A_f)(W_a - W_{s,fb}) \quad (12)$$

where ϕ_{lat} is the latent-heat-transfer fin efficiency, which will be analyzed in the following section.

Meanwhile, the latent-heat-transfer rate δQ_{lat} can be determined.

$$\delta Q_{lat} = \frac{\alpha_{a,sen} \cdot i_{fg}}{C_{p,a} Le^{1-n}} (\delta A_t + \phi_{lat} \cdot \delta A_f)(W_a - W_{s,fb}) \quad (13)$$

2.3. Wet fin efficiency

To solve the above air-side governing equations, wet fin efficiencies are needed [12,13]. In literature, overall fin efficiency that is obtained by the McQuiston method [1,2], is commonly used in the calculation of sensible and latent-heat-transfer rates [3,11]. The following mass transfer equation is used:

$$\delta m_a W_{a2} = \delta m_a W_{a1} - \frac{\alpha_{a,sen}}{C_{p,a} Le^{1-n}} (\delta A_t + \phi \cdot \delta A_f)(W_a - W_{s,fb}) \quad (14)$$

In this study, the overall fin efficiency ϕ is obtained from its definition.

$$\phi = \frac{\delta Q_f}{\delta Q_{\max,f}} = \frac{\phi \left[\alpha_{a,sen}(T_a - T_f) + \frac{\alpha_{a,sen} \cdot i_{fg}}{Le^{1-n} \cdot C_{p,a}} (W_a - W_{s,f}) \right] \cdot dA_f}{\left[\alpha_{a,sen}(T_a - T_{fb}) + \frac{\alpha_{a,sen} \cdot i_{fg}}{Le^{1-n} \cdot C_{p,a}} (W_a - W_{s,fb}) \right] \cdot \delta A_f} \quad (15)$$

Hence

$$Q_f = \phi \cdot A_f \left[\alpha_{a,sen}(T_a - T_{fb}) + \frac{\alpha_{a,sen} \cdot i_{fg}}{Le^{1-n} \cdot C_{p,a}} (W_a - W_{s,fb}) \right] \quad (16)$$

In some cases, the sensible and latent-heat-transfer rates on the fins need to be analyzed separately, that is:

$$Q_f = Q_{sen} + Q_{lat} \quad (17)$$

Due to the unavailability of data, Oskarsson et al. [3] used the overall fin efficiency to calculate the sensible and latent heat transfers respectively:

$$Q_{sen} = \phi \cdot \alpha_{a,sen} A_f (T_a - T_{fb}) \quad (18)$$

$$Q_{lat} = \phi \cdot \alpha_{a,m} A_f i_{fg} (W_a - W_{s,fb}) \quad (19)$$

In other word, the first term in the Eq (16) is regarded as the sensible-heat-transfer rate and the second term as the latent-heat-transfer rate.

It is important to note that the sensible-heat-transfer fin efficiency is not equal to the latent-heat-transfer fin efficiency or the overall fin efficiency. To analyze the sensible and latent heat transfers on the fins, the sensible-heat-transfer fin efficiency and the latent-heat-transfer fin efficiency are introduced in this paper. The latent-heat-transfer fin efficiency ϕ_{lat} is defined as:

$$\phi_{lat} = \frac{\delta Q_{lat,f}}{\delta Q_{lat,\max,f}} = \frac{\phi \alpha_{a,m} \cdot i_{fg}(W_a - W_{s,f}) \cdot dA_f}{\alpha_{a,m} \cdot i_{fg}(W_a - W_{s,fb}) \cdot \delta A_f} \quad (20)$$

Although the air-side governing equations (11) and (12) look simple, the complexity of the heat and mass transfers on the fins is in fact embedded in the solution of Equations (15) and (20).

For better understanding, the sensible-heat-transfer fin efficiency is introduced as follows:

$$\phi_{sen} = \frac{\delta Q_{sen,f}}{\delta Q_{sen,\max,f}} = \frac{\phi \alpha_{a,sen}(T_a - T_f) \cdot dA_f}{\alpha_{a,sen}(T_a - T_{fb}) \cdot \delta A_f} \quad (21)$$

The relationships among the overall, sensible-heat-transfer and latent-heat-transfer fin efficiencies are:

$$\phi = \frac{Q_{sen,f} + Q_{lat,f}}{Q_{sen,\max,f} + Q_{lat,\max,f}} = \frac{Q_{sen,\max,f}}{Q_{sen,\max,f} + Q_{lat,\max,f}} \phi_{sen} + \frac{Q_{lat,\max,f}}{Q_{sen,\max,f} + Q_{lat,\max,f}} \phi_{lat} \quad (22)$$

It can be observed that the overall fin efficiency ϕ is the weighted average of sensible-heat-transfer fin efficiency ϕ_{sen} and the latent-heat-transfer fin efficiency ϕ_{lat}.

With the sensible-heat-transfer and latent-heat-transfer fin efficiencies, the sensible and latent-heat-transfer rates of the wet fin are:

$$\delta Q_{sen,f} = \delta Q_{sen,\max,f} \cdot \phi_{sen} \quad (23)$$

$$\delta Q_{lat,f} = \delta Q_{lat,\max,f} \cdot \phi_{lat} \quad (24)$$

Therefore,

$$\delta Q_f = \delta Q_{sen,\max,f} \cdot \phi_{sen} + \delta Q_{lat,\max,f} \cdot \phi_{lat} \quad (25)$$

Therefore, the latent-heat-transfer rate obtained by Equations (12) and (14) are not identical due to the differences between the overall and latent-heat-transfer fin efficiencies.

To determine the fin efficiencies, the 1-D numerical fin efficiency model presented by Liang et al. [11] are quoted below.

In literature, the fin efficiency of a plate-fin-tube heat exchanger is often approximated by a one-dimensional equivalent circular fin having the same fin area. For circular fins, shown in Fig. 2, the following heat balance equations are solved numerically to obtain the fin temperature distribution.

$$r \cdot \frac{d^2 T_f}{dr^2} + \frac{dT_f}{dr} - r \cdot \frac{2\alpha_{a,sen}}{k_f \cdot t} \cdot (T_f - T_a) = 0 \quad \text{dry fin area} (T_f > T_{d,a}) \quad (26a)$$

$$r \cdot \frac{d^2 T_f}{dr^2} + \frac{dT_f}{dr} - \frac{2r\alpha_{a,sen}}{k_f \cdot t} \cdot \left[(T_f - T_a) + \frac{i_{fg}}{Le^{1-n} \cdot C_{p,a}} (W_{s,f} - W_a) \right] = 0 \quad \text{wet fin area} (T_{d,a} \geq T_f) \quad (26b)$$

Boundary conditions:

$$T_f|_{r=r_i} = T_{fb}; \quad \left. \frac{dT_f}{dr} \right|_{r=r_o} = 0 \quad (27)$$

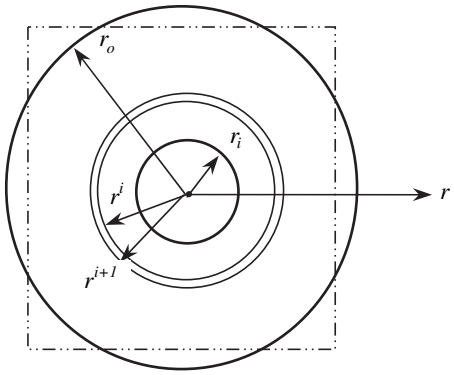

Fig. 2. Schematic diagram of a circular fin having a same surface area as the fin cell shown in Fig. 1b.

The relationship between specific humidity and temperature at saturated conditions is given by a polynomial expression obtained from regression analysis.

$$W_{s,f} = (3.7444 + 0.3078T_f + 0.0046T_f^2 + 0.0004T_f^3) \times 10^{-3} \quad 0 \le T_f \le 30\,^{\circ}\mathrm{C} \tag{28}$$

This is known as a boundary-value problem. The fourth-order Runge–Kutta method is used to solve the above nonlinear differential equation. After the fin temperature distribution is obtained, the fin efficiencies can be calculated.

$$\phi = \frac{\sum_i^N \left[\alpha_{a,sen}(T_a - T_f^i) + \frac{\alpha_{a,sen}\cdot i_{fg}}{Le^{1-n}\cdot C_{p,a}}(W_a - W_{s,f}^i)\right]\cdot\left[(r^{i+1})^2 - (r^i)^2\right]}{\left[\alpha_{a,sen}(T_a - T_{fb}) + \frac{\alpha_{a,sen}\cdot i_{fg}}{Le^{1-n}\cdot C_{p,a}}(W_a - W_{s,fb})\right]\cdot(r_o^2 - r_i^2)} \tag{29}$$

$$\phi_{lat} = \frac{\sum_i^N \alpha_{a,m}\cdot i_{fg}(W_a - W_{s,f}^i)\cdot\left[(r^{i+1})^2 - (r^i)^2\right]}{\alpha_{a,m}\cdot i_{fg}(W_a - W_{s,fb})\cdot(r_o^2 - r_i^2)} \tag{30}$$

$$\phi_{sen} = \frac{\sum_i^N \alpha_{a,sen}(T_a - W_f^i)\cdot\left[(r^{i+1})^2 - (r^i)^2\right]}{\alpha_{a,sen}(T_a - T_{fb})\cdot(r_o^2 - r_i^2)} \tag{31}$$

where $W_{s,f}^i$ is determined by the fin temperature T_f^i using Equation (28).

Case study is conducted to demonstrate the difference among the three fin efficiencies. The sensible-heat-transfer coefficient and the fin maximum possible heat transfer rate are calculated according to the given fin geometric parameters.

The fin geometric parameters and flow conditions are given in Table 1. In the computation, a constant sensible-heat-transfer coefficient is employed over the fin surface. The heat transfer coefficient is determined using the correlation proposed by McQuiston [14]. In literature, a Lewis number value in the range of 0.9–1.0 is assumed for model that employs fin efficiencies and for most traditional cooling models [1,3,15]. Zhou et al. [16] reported that air-water vapor mixture have a Lewis number of around 0.9 at atmospheric conditions for a wide range of temperature and humilities. Thus in this study, an average value of 0.95 is used.

Table 1
Geometric parameters and flow conditions.

Fin geometric parameters	Values	Flow conditions	Values
Width	25 mm	Air velocity	2 m s^{-1}
Height	25 mm	Air inlet relative humidity	20–95%
Fin inner radius	4.76 mm	Air inlet temperature	28 °C
Fin pitch	2.5 mm	Fin base temperature	7.2 °C
Fin thickness	0.12 mm	Fin conductivity	220 W m^{-1} °C

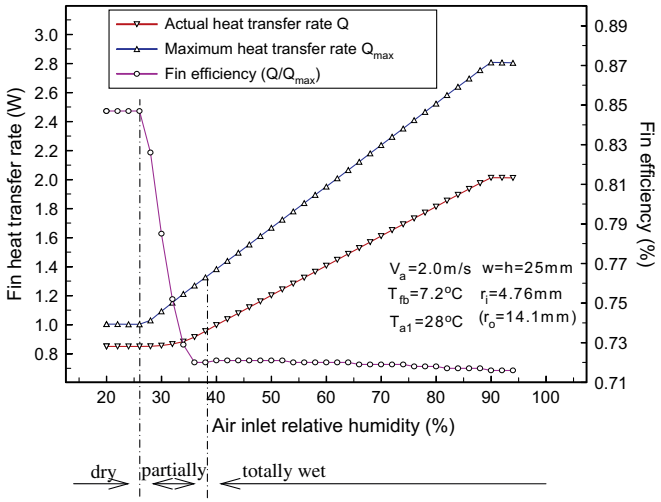

Fig. 3. Overall fin efficiency and fin heat-transfer rate.

Fig. 3 shows that for a given inlet air dry-bulb temperature and fin base temperature, the fin may work in dry condition, partially wet condition and totally wet condition depending on the air inlet relative humidity. For a partially wet fin, the fin efficiency decreases rapidly with the increase in air inlet relative humidity. For a totally wet fin, the effect of the air inlet relative humidity on the fin efficiency is small. To explain this characteristic, the predicted result is examined.

From the variation of fin heat transfer rate with air inlet relative humidity, it is seen that for the given flow conditions, the partially wet fin appears when the air inlet relative humidity is in the range of 26–38%. The results show that for a partially wet fin, both the actual heat transfer rate and maximum possible heat transfer rate increase with the air inlet relative humidity, but the maximum heat transfer rate increases much more rapidly than the actual heat transfer rate. This is because in the maximum possible heat transfer rate calculation, the entire fin were assumed at the fin base conditions, hence the entire fin is treated as a totally wet fin, whereas in the actual heat transfer rate calculation, the fin is only partially wet. Therefore, the air relative humidity has much more effect on the maximum possible heat transfer rate than on the actual heat transfer rate. For a totally wet fin, the ratio of the actual heat transfer rate to the maximum heat transfer rate remains approximately constant; this explains the slight change of fin efficiency.

It can be observed in Fig. 4 that the overall fin efficiency ϕ is the weighted average of sensible-heat-transfer fin efficiency ϕ_{sen} and latent-heat-transfer fin efficiency ϕ_{lat}. The sensible-heat-transfer fin efficiency and the latent-heat-transfer fin efficiency can be determined from Eqs (21) and (20) after the fin temperature distribution is computed. With the sensible-heat-transfer fin efficiency and the latent-heat-transfer fin efficiency, the sensible-heat-transfer rate and the latent heat transfer on the fins can be readily obtained.

Fig. 4 shows the relationship among the three fin efficiencies. It can be observed that the latent-heat-transfer fin efficiency is generally not equal to the sensible-heat-transfer fin efficiency. The results show that both the sensible-heat-transfer fin efficiency and the latent-heat-transfer fin efficiency are strongly dependent on the air relative humidity. Due to the fact that the overall fin

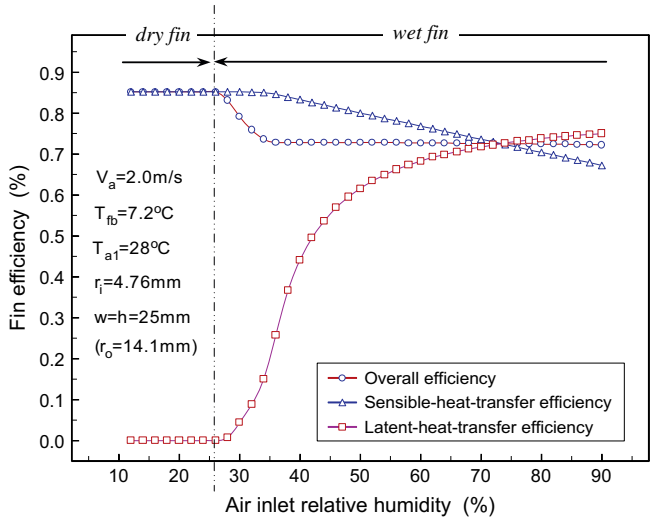

Fig. 4. Overall fin efficiency, sensible-heat-transfer fin efficiency and latent-heat-transfer fin efficiency.

efficiency is the weighted average of sensible-heat-transfer fin efficiency and latent-heat-transfer fin efficiency, the effect of the air humidity on the overall fin efficiency is greatly tempered.

3. Experimental study

A main effort made in this study is to conduct the coil tests under various flow conditions. The experimental data are then used to validate the model predictions. The detail experimental set-up can be obtained from Liang et al. [10].

Experimental data are collected from four evaporator coils using the test rig, shown in Fig. 5. A total of 163 test runs are conducted on four test evaporator coils under a variety of air and refrigerant flow conditions using R134a as the refrigerant. The ranges of the test parameters are as follows:

1) air inlet temperature: from 23 °C to 37 °C,
2) air inlet relative humidity: from 30% to 95%,
3) air coil face velocity: from 1.0 m s^{-1} to 2.8 m s^{-1},
4) refrigerant inlet evaporating temperature: from −2 °C to 17 °C, and
5) refrigerant outlet superheating temperature difference: from 2 °C to 12 °C.

Table 2
Test coil geometric parameters.

Geometric parameters	Values	Geometric parameters	Values
Tube number in each row	8	Inner tube diameter	8.83 mm
Coil face area	0.213 × 0.213 m^2	Fin density	394 m^{-1}
Transverse tube spacing	25 mm	Fin type	Wavy-fin
Longitudinal tube spacing	21.6 mm	Tube arrangement	Stagger
Outer tube diameter	9.53 mm		

The geometric parameters of the test coils are given in Table 2 and the respective refrigerant circuitry arrangements are illustrated in Fig. 6. *Coils 1* and *2* use simple refrigerant circuitry with three and four tube rows respectively. To validate the model for evaporator coils with complex refrigerant circuitry [10], *Coils 3* and *4* are used, where having the same tube number as *Coil 1*, the refrigerant circuits are branched or joined in return bends.

On the air side, the enthalpies and specific humidities at the inlet and outlet of the test coil are calculated from the measured air dry-bulb temperatures and relative humidities at both locations. On the refrigerant side, the enthalpies for single-phase refrigerant are calculated based on the measured temperatures and pressures. The enthalpy of the refrigerant at the inlet of the test coil is determined by the enthalpy at the inlet of the expansion valve, with the assumption of isenthalpic expansion.

The rate of heat transfer by the air is calculated based on the following equation:

$$Q_a = m_a(h_{in,a} - h_{out,a}) - C_{p,a}T_w m_a(W_{in,a} - W_{out,a}) \quad (32)$$

The rate of heat transfer by the refrigerant is calculated based on its enthalpy difference.

$$Q_r = m_r(h_{out,r} - h_{in,r}) \quad (33)$$

The range of the estimated uncertainties of the heat transfer rates on the air side is from 3.94% to 9.97%, whereas the range on the refrigerant side is from 0.68% to 0.8%. It is noted that the uncertainty existing in the air-side measurement is much greater than that in the refrigerant-side measurement. Thus, the coil capacities deduced from the refrigerant-side measurements are used in the ensuing comparison. A comparison of the coil capacities

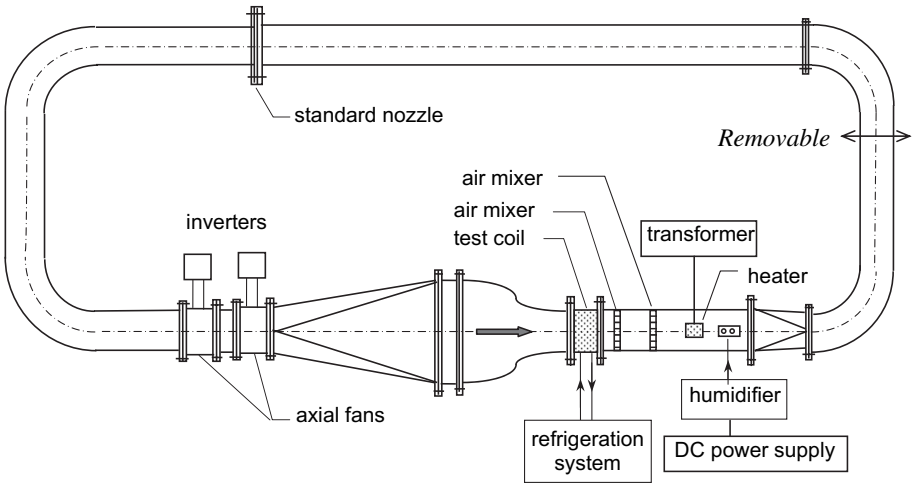

Fig. 5. Schematic of coil test rig.

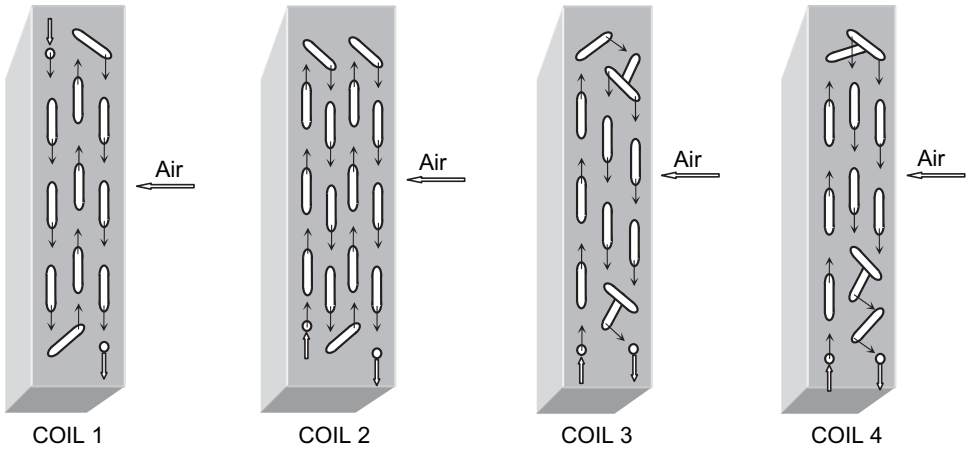

Fig. 6. Return bend connections of four test evaporator coils.

measured from the refrigerant side and the air side is done. Good agreement is obtained with errors less than 3%.

The comparison between the model predictions and the experimental data is presented in term of root-mean-square error (*RMS*) and average error. Depending on whether an error is indicated by a percentage or not, there are two types of error forms, which are respectively defined as:

$$RMS\ error\ I = \left[\frac{1}{N}\sum_{1}^{N}\left(\frac{X_p - X_m}{X_m}\right)^2\right]^{\frac{1}{2}} \times 100\% \tag{34a}$$

$$RMS\ error\ II = \left[\frac{1}{N}\sum_{1}^{N}(X_p - X_m)^2\right]^{\frac{1}{2}} \tag{34b}$$

$$Average\ error\ I = \frac{1}{N}\sum_{1}^{N}\left(\frac{X_p - X_m}{X_m}\right) \times 100\% \tag{35a}$$

$$Average\ error\ II = \frac{1}{N}\sum_{1}^{N}(X_p - X_m) \tag{35b}$$

where X is the parameter of interest, *e.g.* coil capacity. Generally, the errors of coil capacity and pressure drop are presented using type I form, while the errors of air outlet temperature, relative humidity and the refrigerant outlet temperature are presented using type II form.

The *RMS* error gives the arithmetic mean absolute error of the data. The average error may sometimes give exaggerated agreement due to the canceling of positive and negative prediction errors but does give a general indication of over and under prediction.

4. Comparison

To simulate a coil with complex refrigerant circuitry, the approach proposed by the author (Liang et al. [10]) is employed. In evaporator modeling, correlations are needed to determine the heat transfer coefficients and pressure drops, which include the air-side sensible-heat-transfer coefficient, air-side pressure drop, refrigerant-side single-phase and evaporating heat transfer coefficients and refrigerant-side pressure drop. Thus, it is necessary to choose appropriate correlations in order to increase the accuracy of the proposed model. As there are numerous existing correlations, it is almost impossible to test every possible combination of the correlations.

On the refrigerant side, the commonly used correlation proposed by Jung et al. [17] is employed for the evaporating heat transfer coefficient. This correlation, initially based on the experimental data obtained with R22, R12, R152a, and R114, was further validated by comparing it with R134a experimental data [18,19]. Meanwhile, the friction multiplier correlation and the loss factor for return bends by Paliwoda [20,21] are used for pressure drop predictions on the refrigerant side.

The air-side sensible-heat-transfer coefficient correlations used in the model prediction tested against the experimental data are listed below:

1) Elmahdy and Biggs correlation [23],
2) McQuiston correlation [14], and
3) Gray and Webb correlation [22]

In literature, the method proposed by McQuiston [1] for the wet fin efficiency is widely used to the plate-fin-tube heat exchangers [2]. However, this method assumes that the latent-heat-transfer fin efficiency equals to the overall fin efficiency. Attempt has been made to compare the McQuiston method with the proposed 1-D numerical model.

Figs. 7–10 present comparison between the measured experimental data (coil cooling capacity, refrigerant outlet temperature, air dry-bulb temperature and relative humidity at the outlet of the coils)

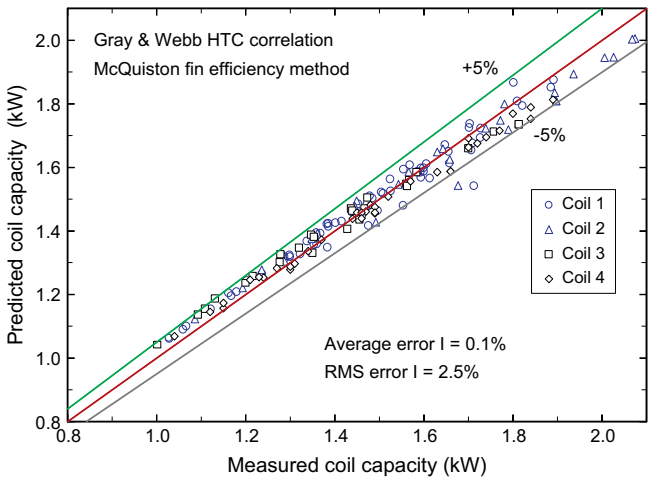

Fig. 7. Comparison of predicted coil capacity with the experimental measurement.

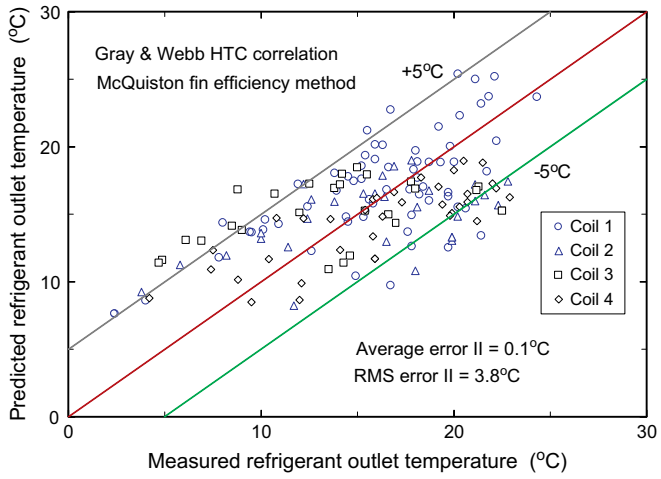

Fig. 8. Comparison of predicted refrigerant outlet temperature with the experimental measurement.

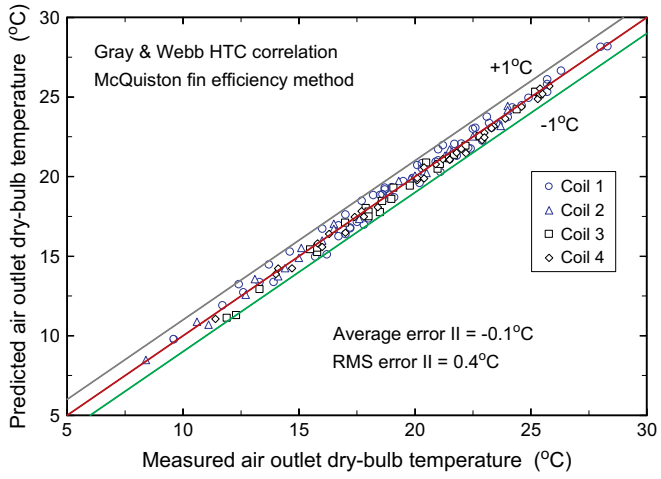

Fig. 9. Comparison of predicted air outlet dry-bulb temperature with the experimental measurement.

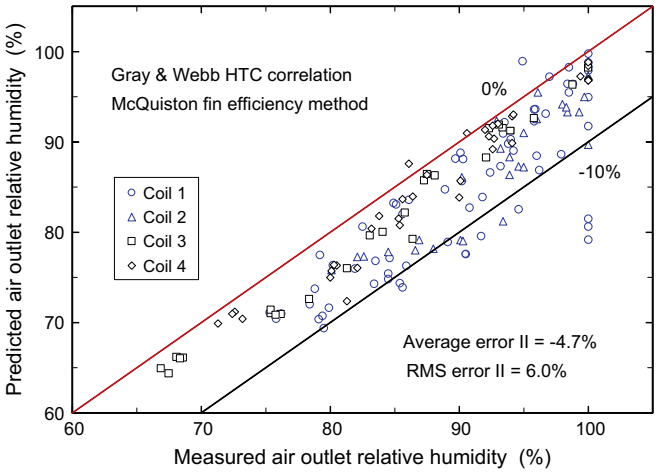

Fig. 10. Comparison of predicted air outlet relative humidity with the experimental measurement.

Table 3
The average and *RMS* errors of the evaporator model predictions.

Parameters	(a) Sensible *HTC* McQuiston correlation; ϕ: McQuiston method [2]; ϕ_{lat}: McQuiston method [2]		(b) Sensible *HTC* Gray and Webb correlation; ϕ: McQuiston method [2]; ϕ_{lat}: McQuiston method [2]		(c) Sensible *HTC* Gray and Webb correlation; ϕ: Equation (29); ϕ_{lat}: Equation (30)	
	Average	*RMS*	Average	*RMS*	Average	*RMS*
Q	0.02%	2.5%	0.1%	2.5%	0.4%	2.1%
$T_{r,out}$	−0.04 °C	3.8 °C	0.1 °C	3.8 °C	0.1 °C	2.9 °C
$T_{a,out}$	−0.1 °C	0.4 °C	−0.1 °C	0.4 °C	−0.2 °C	0.4 °C
$Rh_{a,out}$	−4.8%	6.1%	−4.7%	6.0%	−0.5%	3.5%

and the model predictions using Gray and Webb sensible-heat-transfer correlation in conjunction with McQuiston wet fin efficiency. For most test cases, the coil capacity can be predicted with an error within ±5%, refrigerant outlet temperature within ±5 °C, air outlet dry-bulb temperature within ±1 °C, and air outlet relative humidity with 0% to −10%.

The average errors and the *RMS* errors of the model predictions using McQuiston sensible-heat-transfer correlation in conjunction with McQuiston wet fin efficiency against the experimental data are given in Table 3a. The results indicate that there is no significant difference among the model predictions when various sensible air-side *HTC* correlations are used (Table 3a,b), it is also noted that the same results are obtained when using the Elmahdy and Biggs correlation. The results highlight that the model is insensitive to the air-side sensible-heat-transfer coefficients when the refrigerant-side conditions are specified. Hence, using various *HTC* correlations will not improve the model accuracy.

To validate the modified model on the air side, the 1-D numerical model for latent-heat-transfer and overall-heat-transfer fin efficiency presented above is used in the evaporator modeling. Figs. 11–14 are the corresponding comparison using the Gray and Webb sensible *HTC* correlation in conjunction with the proposed numerical fin efficiency model. The average errors and the *RMS* errors of the model predictions against the experimental data are collected in Table 3c. The results indicate that the evaporator model gives a better prediction when the proposed numerical latent-heat-transfer and overall-heat-transfer fin efficiency model is used.

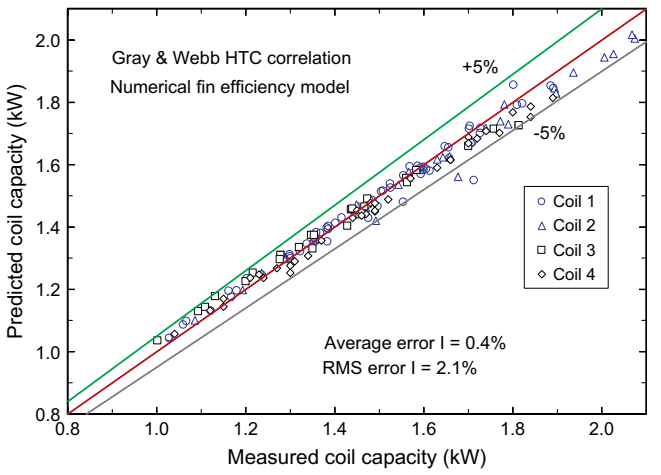

Fig. 11. Comparison of predicted coil capacity with the experimental measurement (1-D numerical fin efficiency model).

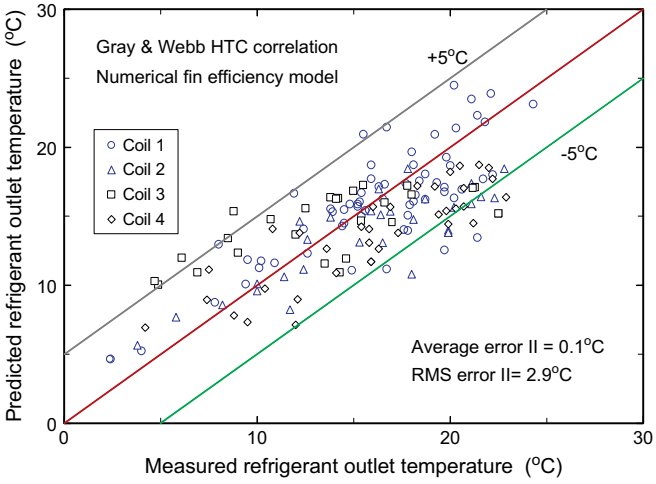

Fig. 12. Comparison of predicted refrigerant outlet temperature with the experimental measurement (1-D numerical fin efficiency model).

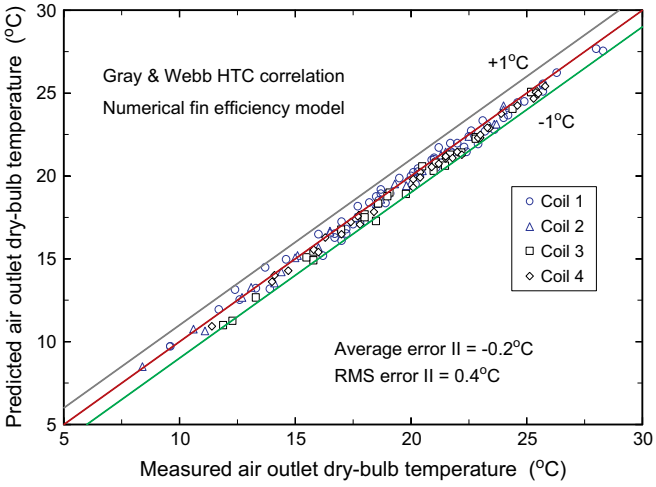

Fig. 13. Comparison of predicted air outlet dry-bulb temperature with the experimental measurement (1-D numerical fin efficiency model).

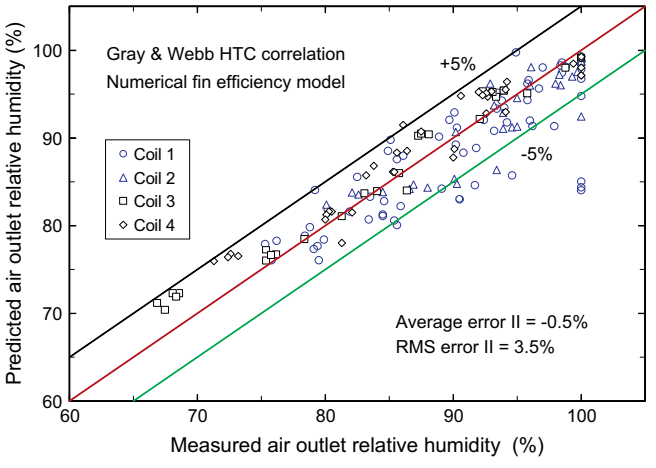

Fig. 14. Comparison of predicted air outlet relative humidity with the experimental measurement (1-D numerical fin efficiency model).

To investigate the accuracy of the proposed theoretical model, the outlet refrigerant temperature is chosen for comparison, as shown in Figs. 8 and 12. It is noted that among the predicted parameters (cooling capacity, refrigerant outlet temperature, air-side outlet dry-bulb temperature and relative humidity), the refrigerant outlet temperature is the most sensitive parameter. As the coil capacity is the product of refrigerant mass flow rate and enthalpy difference between inlet and outlet, the refrigerant outlet temperature is closely related to the coil capacity when the refrigerant mass flow rate and the inlet enthalpy are specified. A small change on the coil capacity will result in a greater variation in the outlet refrigerant temperature due to the low specific heat of the superheating refrigerant. Compared with Fig. 8, it can be seen from Fig. 12 that the mean deviation of the refrigerant outlet temperature prediction against the measured results is significantly decreased after using the 1-D numerical fin efficiency model. Moreover, in comparison of Fig. 10 with Fig. 14, it is observed that the model accuracy of predicting the air outlet relative humidity is significantly increased after using the numerical fin efficiency model. The average error is reduced from −4.7% to −0.5% and the *RMS* error is reduced from 6.0% to 3.5%. Because the air relative humidity is a function of the air dry-bulb temperature and the moisture content, its accuracy may reflects the model prediction on the sensible heat transfer and latent heat transfer. From the comparison, it is validated that the 1-D numerical fin efficiency model can predict the coil sensible heat transfer and latent-heat-transfer more accurately. The improvement in the prediction of the refrigerant outlet temperature is in fact the result of the improvement in the air-side heat and mass transfer modeling.

The study shows that in evaporator modeling, the approach used to model the wet fin efficiency has a significant effect on the model prediction, while the choice of sensible air-side *HTC* correlation has little effect on the model prediction.

5. Conclusion

To analyze the heat and mass transfer on the wet surface of the evaporator coils, the sensible and latent-heat-transfer fin efficiencies are introduced. It is important to note that the latent-heat-transfer fin efficiency is generally not equal to the sensible-heat-transfer fin efficiency or the overall fin efficiency. The results show that both the sensible-heat-transfer fin efficiency and the latent-heat-transfer fin efficiency are strongly dependent on the air relative humidity. Due to the fact that the overall fin efficiency is the weighted average of sensible-heat-transfer fin efficiency and latent-heat-transfer fin efficiency, the effect of the air humidity on the overall fin efficiency is greatly tempered.

The modified evaporator model has been validated by the extensive comparison of the model predictions against the experimental data on the evaporator coils with various configurations which include the simple and complex refrigerant circuitry. The study shows that the approach used to model the wet fin efficiency has a significant effect on the model prediction. Particularly, the accuracy of the model is significantly improved by the introduction of latent-heat-transfer fin efficiency.

References

[1] F.C. McQuiston, Fin efficiency with combined heat and mass transfer. ASHRAE Trans. 81 (1) (1975) 350–355.
[2] F.C. McQuiston, J.D. Parker, Heating, Ventilating and Air Conditioning, fourth ed. John Wiley & Sons, New York, 1994.
[3] S.P. Oskarsson, K.I. Krakow, S. Lin, Evaporator models for operating with dry, wet and frosted finned surfaces. Part I: heat transfer and fluid flow theory. ASHRAE Trans. 96 (1) (1990) 373–380.

[4] F. Ragazzi, Thermodynamic optimization of evaporators with zeotropic refrigerant mixtures, Ph.D. Dissertation, University of Illinois at Urbana-Champaign, 1995.
[5] Y.K. Chuah, C.C. Hung, P.C. Tseng, Experimental performance of a finned tube heat exchanger. HVAC Res. 4 (1998) 167–178.
[6] K.T. Hong, R.L. Webb, Calculation of fin efficiency for wet and dry fins. HVAC Res. 2 (1996) 27–41.
[7] S.G. Kandlikar, Thermal design theory for compact evaporators. in: R.L. Kraus, et al. (Eds.), Compact Heat Exchanger. Hemisphere Publishing Corp., New York, 1990, pp. 245–286.
[8] G. Wu, T.Y. Bong, Overall efficiency of a straight fin with combined heat and mass transfer. ASHRAE Trans. 100 (1) (1994) 367–374.
[9] S.Y. Liang, T.N. Wong, G.K. Nathan, Comparison of one-dimensional and two-dimensional models for wet-surface fin efficiency of a plate-fin-tube heat exchanger. Appl. Thermal Eng. 20 (2000) 941–962.
[10] S.Y. Liang, T.N. Wong, G.K. Nathan, Numerical and experimental studies of refrigerant circuitry of evaporator coils. Int. J. Refrig. 24 (2001) 823–833.
[11] S.Y. Liang, M. Liu, T.N. Wong, G.K. Nathan, Analytical study of evaporator coil in humid environment. Appl. Thermal Eng. 19 (1999) 1129–1145.
[12] L.T. Chen, Two-dimensional fin efficiency with combined heat and mass transfer between water-wetted fin surface and moving moist airstream. Int. J. Heat Fluid Flow 12 (1991) 71–76.
[13] Y.T. Lin, K.C. Hsu, Y.J. Chang, C.C. Wang, Performance of rectangular fin in wet conditions: visualization and wet fin efficiency. ASME J. Heat Transf. 123 (2001) 827–836.
[14] F.C. McQuiston, Finned tube heat exchangers: state of the art for the air side. ASHRAE Trans. 87 (1) (1981) 1077–1085.
[15] J.L. Threlkeld, Thermal Environmental Engineering, second ed. Prentice Hall, Englewood Cliffs, NJ, 1970.
[16] X. Zhou, James E. Braun, Q. Zeng, An improved method for determining heat transfer fin efficiencies for dehumidifying cooling coils. HVAC Res. 9 (2007).
[17] D.S. Jung, M. McLinden, R. Radermacher, D. Didion, A study of flow boiling heat transfer with refrigerant mixtures. Int. J. Heat Mass Transf. 32 (9) (1989) 1751–1764.
[18] D.S. Jung, R. Radermacher, Prediction of heat transfer coefficients of various refrigerants during evaporation. ASHRAE Trans. 97 (2) (1991) 48–53.
[19] J. Judge, R. Radermacher, A heat exchanger model for mixtures and pure refrigerant cycle simulations. Int. J. Refrig. 20 (1997) 244–255.
[20] A. Paliwoda, Generalized method of pressure drop and tube length calculation with boiling and condensing refrigerants within the entire zone of saturation. Int. J. Refrig. 12 (1989) 314–322.
[21] A. Paliwoda, Generalized method of pressure drop calculation across pipe components containing two-phase flow of refrigeration. Int. J. Refrig. 15 (1992) 119–124.
[22] D.L. Gray, R.L. Webb, Heat transfer and friction correlations for plate finned-tube heat exchangers having plain fins, in: Proceedings of the Eight International Heat Transfer Conference, San Francisco, vol. 6, 1986, pp. 2745–2750
[23] A.H. Elmahdy, R.C. Biggs, Finned tube heat exchanger correlation of dry surface heat transfer data. ASHRAE Trans. 85 (2) (1979) 252–273.